Journal of Coastal Research	34	5	1021–1034	Coconut Creek, Florida	September 2018

Seabed Attributes and Meiofaunal Abundance Associated with a Hydrodynamic Gradient in Baynes Sound, British Columbia, Canada

Terri F. Sutherland[†]*, Lorena M. Garcia-Hoyos[†], Perry Poon[†], Maxim V. Krassovski[‡], Michael G.G. Foreman[‡], Alan J. Martin[§], and Carl L. Amos[††]

[†]Fisheries and Oceans Canada
Pacific Science Enterprise Centre
West Vancouver, BC V7V 1N6, Canada

[‡]Fisheries and Oceans Canada
Institute of Ocean Sciences
Sidney, BC V8L 5T5, Canada

[§]Lorax Environmental Services
Vancouver, BC V6J 3H9, Canada

[††]National Oceanography Centre
University of Southampton
Southampton SO14 3ZH, England, U.K.

www.cerf-jcr.org

www.JCRonline.org

ABSTRACT

Sutherland, T.F.; Garcia-Hoyos, L.M.; Poon, P.; Krassovski, M.V.; Foreman, M.G.G.; Martin, A.J., and Amos, C.L., 2018. Seabed attributes and meiofaunal abundance associated with a hydrodynamic gradient in Baynes Sound, British Columbia, Canada. *Journal of Coastal Research,* 34(5), 1021–1034. Coconut Creek (Florida), ISSN 0749-0208.

The distribution of seabed geotechnical, biochemical, and meiofauna attributes was examined in Baynes Sound, British Columbia, between 2009 and 2014. Among attributes measured were sediment porosity, organic carbon and nitrogen, and trace element concentrations (*e.g.*, zinc, copper), which increased with increasing sediment fines content toward the head of the Sound. A ternary plot (sand-silt-clay percentages) revealed a constant clay/silt ratio across a range of sand proportions with textures ranging from well-sorted sand at the high-energy SE entrance to silt-dominated mud in the depositional basin. These sediment textures were related to modeled maximum velocity values within 5 m of the seabed ($U_{max,5}$), with highest values (restricted entrance) and lowest values (deep basin) representing sand depositional and mud depositional facies. Sediment porewater sulfide fell into an oxic category (0–700 μM), exhibiting a lack of variation and organic enrichment within the Sound. The first principal component analysis (PCA) factor described the alignment between fine sediments, organics, Cu and Zn, and meiofauna attributes and accounted for 49% of the total variance. The second PCA factor (19% of total variance) described the relationship between $U_{max,5}$ and sediment grain size fractions >0.5 mm and an indirect association with water depth and fine sand (0.105–0.250 mm). Meiofauna were associated with a medium sand fraction (0.25 mm) characterized by low-porosity and low-organic sand loam textures. Although the range in abundance was relatively greater for nematodes, harpacticoid copepods revealed a stronger response to changes in sediment geotechnical and organic attributes, suggesting these taxa may be used to describe seabed variations or potential perturbations.

ADDITIONAL INDEX WORDS: *Sediment, texture, porosity, meiofauna, nutrients, velocity.*

INTRODUCTION

Estuaries are highly productive elements of the coastal zone, being exposed to both freshwater and marine influences that support diverse habitats and species assemblages (Arai and Hay, 1982; Bravender *et al.*, 2002; Dawe, Buechert, and Trethewey, 1998; Forrester and Ketchen, 1963; Jenkins *et al.*, 2006). The complex nature of estuaries is further enhanced by the influences of river flow, tides, waves, and wind, which influence flow velocity, water temperature, salinity, and turbidity, with consequent effects on sediment transport and seabed sediment texture: These influences operate on diurnal, tidal, seasonal, and interannual time scales (Fairbridge, 1980). Estuaries accumulate fine particles that come from terrestrial, river-born, marine, atmospheric, and anthropogenic sources (Liu *et al.*, 2010; Noronha-D'Mello and Nayak, 2015; Vilas, Bemabeu, and Mendez, 2005; Volvoikar and Nayak, 2013; Volvoikar *et al.*, 2014). Particle trapping is a characteristic feature of estuaries with shallow sills, restricted entrances, a significant estuarine turbidity maximum (ETM), or a combination of factors (Jay and Musiak, 1994). Spatial patterns in particle deposition and seabed texture reflect processes governed by hydrodynamic, depositional, and floc-forming conditions (Molinaroli *et al.*, 2009; Pejrup, 1988). In this regard, seabed characterization is important because sediment texture, and its relationship to organic matter carbon accumulation and nutrient recycling, has a significant role in biogeochemical processes and habitat suitability (Dessai, 2008; Sutherland *et al.*, 2007a,b).

Sediment texture has environmental significance in terms of its habitat function based on its close association with organic enrichment and meiofaunal communities (Duplisea and Hargrave, 1996; Heip, Vincx, Vranken, 1985). Meiofauna play an important role in the food web by serving as a food source for macrofauna and fish (Carpentier *et al.*, 2014; Forrester and Ketchen, 1963; Webb, 1991) as well as a consumer of microbes, microphytobenthos, and detritus (Mascart *et al.*, 2015; Montagna *et al.*, 1983; Torres-Pratts and Schizas, 2007). The meiofauna size fraction (63–500 μm) largely makes up an interstitial niche where they exploit seabeds dominated by

DOI: 10.2112/JCOASTRES-D-17-00213.1 received 14 December 2017; accepted in revision 6 February 2018; corrected proofs received 12 March 2018; published pre-print online 10 April 2018.
*Corresponding author: Terri.Sutherland@dfo-mpo.gc.ca

variations in sand-silt-clay ratios (Fenchel, 1969; Schwinghamer, 1981). It is well known that meiofauna respond to (1) sediment physical structure and disturbances (Coull and Chandler, 1992; Heip, Vincx, and Vranken, 1985; Liu *et al*., 2015; Schratzberger and Warwick, 1998a; Warwick and Buchanan, 1970), (2) benthic organic enrichment (Amjad and Gray, 1983; Mirto *et al*., 2000; Sundulli and De Nicola, 1991; Sutherland *et al*., 2007a), and (3) hypoxic or anoxic events (Diaz and Rosenberg, 1995; Murrell and Fleeger, 1989; Steyaert *et al*., 2007). Given their small size, interstitial status, short life cycle, and response to physical and biogeochemical perturbations, meiofauna are considered a valued component when characterizing seabeds (Coull and Chandler, 1992; Higgins and Thiel, 1988). Overall, understanding the spatial variation in sediment textures and geotechnical attributes in estuaries is important because the seabed is a key habitat for various infaunal taxa that provide an important food source in higher trophic levels in the food web (Coull, Hicks, and Wells, 1981).

The objective of this project was to study the distribution and abundance of sediment components and meiofaunal taxa in relation to a hydrographic gradient (NW–SE axis) along the length of Baynes Sound (BS). Sediment variables, including sediment grain size, porosity, organic carbon, organic nitrogen, porewater sulfide, redox potential, and trace-elements (Cu and Zn) were considered in this study because they (1) are known to respond to hydrodynamic forces and influence faunal communities and (2) represent indicators of potential benthic organic enrichment processes (Hargrave, Holmer, and Newcombe, 2008; Holmer *et al*., 2005; Sutherland *et al*., 2007a,b; Wildish, Hargrave, and Pohle, 2001). In terms of meiofaunal taxa, nematodes and harpacticoid copepods were examined because they (1) tend to dominate total meiofaunal abundance (Heip, Vincx, Vranken, 1985; Liu *et al*., 2015; Neira *et al*., 2001; Sundulli and De Nicola Giudici, 1989; Vidakovic, 1983) and (2) have been shown to respond to sediment texture and organic enrichment gradients (Mirto *et al*., 2000; Sun *et al*., 2014; Sutherland *et al*., 2007a). In this manner, nematodes (Phylum: Nematoda) and harpacticoid copepods (Copepoda: Harpacticoidea) were examined to determine their response to varying sediment properties along a hydrodynamic gradient. This study provides the first characterization of subtidal sediments in BS and is part of a larger project assessing the carrying capacity of shellfish aquaculture in the Sound.

Study Site

Baynes Sound is a coastal embayment located in the northern Strait of Georgia and is bordered by both Vancouver Island and Denman Island, British Columbia (Figure 1). It has a length of 40 km that runs along a NE–SW axis, an average width of 2.2 km, and an area of 90 km^2. BS follows Pritchard's (1967) estuarine definition of a semienclosed waterbody that exchanges with the open sea and is diluted by fresh water from terrestrial inflows. The Courtenay River (mean annual discharge: 51.3 m^3s^{-1}; Riddell and Bryden, 1996) is formed by two tributaries, the Tsolum and Puntledge rivers, and provide the largest input of freshwater runoff that drives a two-layer estuarine circulation within the Sound. BS is unique and differs from other local estuaries or fjords in that it has two locations where water can exchange with the ocean. BS exchanges water with that of the Strait of Georgia at two locations (Figure 1): (1) the NE Comox Bar connecting Denman Island and Comox and (2) the SW entrance between Maple-guard and Repulse points. The Comox Bar limits water exchange within the top 4 m of the water column, whereas the SW entrance is the primary conduit for tidal exchanges across a 1-km-wide and 20-m-deep channel. The upper reach of BS consists of a depositional basin bordered by Vancouver Island, Courtenay River estuary, and the Comox sandbar and is influenced by both the Courtenay River and marine inputs across the Comox Bar. Sediment dispersal consists of the transport of (1) coarse sediment limited to the sandbar and shorelines and (2) fine sediment extending farther down the shoreline slopes and across the basin (Clague, 1976). As a result, this basin is characterized by fine-grained sediment in deep water, silty sand on the shoreline slopes, and gravelly sand on the river delta and sandbar connecting Comox to Denman Island, respectively. The middle reach consists of a narrow channel between Denman Island and both the Base Flat and Ship's Peninsula, connecting the upper and lower reaches of BS. The lower reach widens to include both Mud and Deep bays on the SE border and then narrows across the subtidal bar located inside the restricted entrance of the Sound.

Extensive tidal flats (the result of a 4–5-m spring tidal range) exist in the (1) upper reach at Comox Flats, Comox Bar, and White Spit; (2) middle reach at Base Flat, Fanny Bay, and Ships Point; and (3) lower reach at Mud Bay and Deep Bay (Figure 1). The vast intertidal zone, extensive NE sandbar, and sheltered estuary provide important staging, breeding, and overwintering sites for local and migratory birds (Carswell, Cheesman, and Anderson, 2006; Jamieson *et al*., 2001; Lacroix *et al*., 2005). BS supports Pacific salmon at various stages of their life histories, is a significant herring spawning habitat, and accounts for a significant proportion of shellfish aquaculture production in British Columbia, Canada (Arai and Hay, 1982; Bravender *et al*., 2002; Dawe, Buechert, and Trethewey, 1998; Jenkins *et al*., 2006).

METHODS

Sediment samples were collected between 2009 and 2014 over the spring-summer season (19 April 2009, 11 April and 11 August 2011, 8 July 2012, 9 April and 20 June 2014). Sampling stations 1–21 were located within BS proper, and stations 22 and 23 were located outside the south entrance (Figure 1). Within the Sound, the nearshore stations were located on the 20-m bathymetric contour to standardize sampling of station water depths. The water depths of the central stations that followed the N–S axis naturally increased toward the head of the Sound. A Smith-McIntyre grab with a sediment surface area of 0.1 m^2 was used to collect both sediment and meiofauna samples (Gage and Bett, 2007).

After retrieval of a grab, the top doors were opened and the water was allowed to drain off the sediment surface. Sediment was collected from the uppermost 2 cm of the sediment sample immediately after the overlying water was gently drained from the grab. At each station, a 500-mL sediment sample was collected for grain size analysis, and a 100-mL sediment sample was taken for the analysis of sediment porosity, total organic carbon, total organic nitrogen content, and trace element

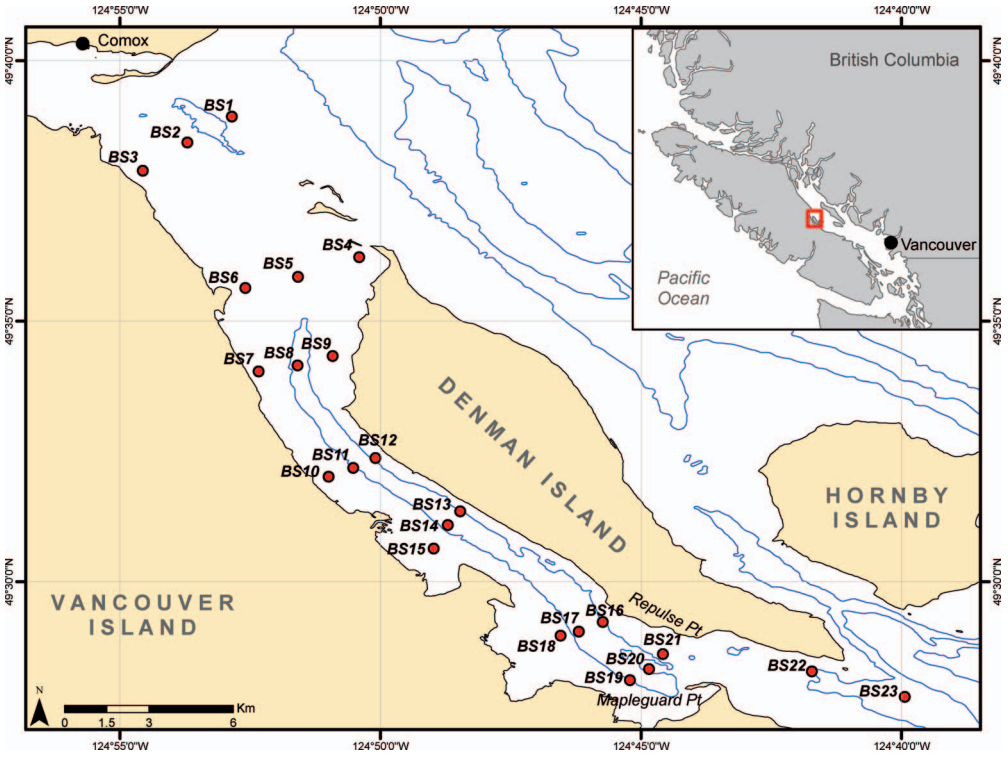

Figure 1. Location of sampling stations in Baynes Sound, British Columbia, Canada.

concentrations. These samples were frozen for storage and transport to the laboratory. Samples were treated with sodium hypochlorite (NaOCl) to remove organic material before sediment grain size fractionation. Thereafter, the bulk sediment sample was wet sieved to separate sand (>63 μm) from finer material (silt and clay). The sand was sieved into six size classes; the fine silt and clays were analyzed following the pipette method (McKeague, 1978). The following grain size categories were reported on a dry weight basis: >2000 μm, <2000 μm, <1000 μm, <500 μm, <250 μm, <100 μm, <63 μm, <4 μm, <2 μm. Textural classes were expressed as sand, silt, and clay proportions with the silt-clay boundary (0.002 mm) set according to the Canadian System of Soil Classification (Soi1 Classification Working Group, 1998). Sediment grain size statistics were computed as follows: (1) the phi unit corresponds to the median or the 50th percentile mark on a cumulative curve, where one-half of the particle weight is larger than the median and the other half smaller; (2) sorting and skewness statistical parameters were calculated using GRADISTAT-8 (Blott, 2010) according to the descriptive method of moments outlined in Folk and Ward (1957). Water content (percentage by mass) was calculated using the differential weight values between wet and dry measurements standardized by wet weight. After wet weight determination, sediment was dried at 55°C for 48 hours and desiccated for 2 hours.

The hydrodynamics of BS have been simulated using the Finite Volume Community Ocean Model (FVCOM; Chen, Liu, and Beardsley, 2003). The model was forced with tides, river discharges, winds, and heat flux exchanges with the atmosphere. The model currents have been depth-averaged over the bottom 5 m of the water column ($U_{\max,5}$). The maximum hourly values for these depth-averaged currents over the time period from 1 June to 31 August 2012 at the station locations (Figure 1) were used in the analysis.

Carbonate material was removed from sediment samples through acidification. Total organic carbon and nitrogen values were obtained using a Thermo Finnigan FlashEA 1112 coupled to a Thermo Finnigan Delta Plus XL through a ConFlo III. Organic material was oxidized to carbon dioxide, various nitrogen bearing gases, and water. This gas mixture was then passed through a reduction furnace packed with elemental Cu at 680°C to reduce all nitrogen-bearing compounds to pure gaseous nitrogen. The resulting gases were then passed through a water trap to eliminate moisture. A gas chromatography column at 50°C was used to separate the carbon dioxide and nitrogen gases for analysis in the mass spectrometer. The data were blank corrected, and the percent carbon and nitrogen measurements were reported by mass (precision of ±10%).

The analysis of sediment Cu and Zn contents was carried out according to the U.S. Environmental Protection Agency (EPA) method ICP-AES 200.15 for metal and trace element analysis using ultrasonic nebulization (U.S. EPA, 1994). A sediment sample was dried at 55°C until a constant weight was achieved and then passed through a 1-mm sieve. The digestion process follows that of Strong Acid Leachable Metals and was digested

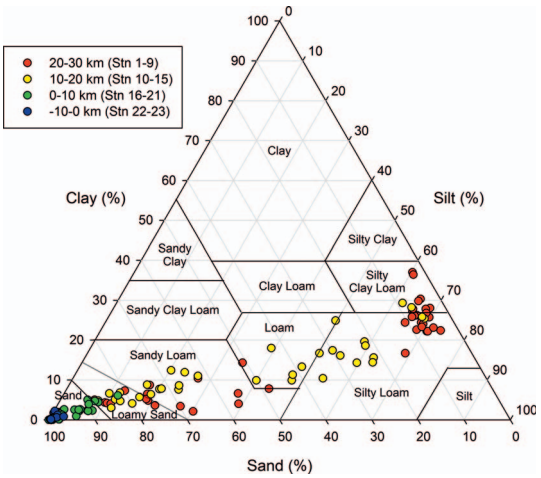

Figure 2. Ternary plot based on proportions of sand, silt, and clay overlaid with substrate texture classifications. The sampling stations color-coded by station distance from the SE entrance of Baynes Sound, British Columbia, show that fine sediments increase toward the head of the Sound.

in a mixture of concentrated nitric and hydrochloric acids at 90°C for 2 hours. The extracts were then analyzed for trace element content via inductively coupled plasma atomic emission spectroscopy (ICP-AES).

A modified 60-mL syringe core (Somerfield, Warwick, and Moens, 2005) was inserted vertically into the uppermost 2 cm of sediments within the grab sample to capture the surficial meiofaunal community. The syringe core subsample was transferred to a 100-mL beaker containing a volume of sulfide antioxidant buffer equal to that of the subsample volume. The subsample was immediately mixed with the buffer solution, and the dissolved sulfide concentration (H_2S, HS^-, S^{2-}; μM) was measured using an Orion silver/sulfide electrode (Orion 6916BN) and an Accumet AP63 portable meter. The silver/sulfide electrode was filled with Optimum results "A" filling solution (Orion 900061) 24 hours before use and calibrated using three solutions made from sodium sulfide nonahydrate with concentrations of 10,000, 1000, and 100 μM. Redox potential E_{NHE} measurements were conducted using an Orion combination platinum redox electrode (Orion 9678BN) in series with an Accumet AP63 portable meter. The redox electrode was filled with a 4 M Ag/AgCl filling solution (Orion 900011) 24 hours before use. ZoBell's A and B solutions were prepared so that the redox electrode could be checked periodically to ensure proper functioning. The Orion probe was inserted directly into the sediment to a depth of 1 cm, a midway point within the top 2 cm, and allowed to equilibrate for a 3-minute period before the redox value was recorded.

The outer core barrel of the modified 60-mL syringe core was deployed vertically into the center of the grab, with the plunger maintained at a position above the water-sediment interface. The bottom end of the syringe core was capped before retrieval of the syringe core from the sediment. The plunger was removed from the top end of the barrel and inserted into the bottom end of the barrel, meanwhile maintaining the syringe core barrel in a vertical orientation. The plunger was used to extrude the uppermost 2 cm of sediment from the barrel and placed in a labeled 50-mL jar, which was then placed in a freezer for storage and transportation to the laboratory. In the laboratory, meiofauna were extracted from each sediment sample following the method of Warwick and Buchanan (1970). Each sediment sample was passed through stacked sieves consisting of 0.5- and 0.063-mm mesh sizes. The sample retained on the 0.063-mm sieve was transferred to a 1000-mL graduated cylinder and filled to a volume of 850 mL with filtered seawater (0.45-μm filter membrane). The sample was suspended in the cylinder and allowed to stand for 60 seconds to allow for the settlement of larger particles. The organisms in the supernatant seawater were retained after they were passed through a 0.063-mm sieve. The procedure of sample resuspension, settlement, and decantation was repeated three more times, resulting in the collection of additional sample material on the 0.063-mm sieve. The entire sample was then scanned under ×10 and ×40 magnification using a Leica Wild M3Z microscope. Rose Bengal was added to the sample to help identify meiofauna within the suspended debris. Meiofauna abundance was standardized to the area of the 60-mL syringe core (barrel diameter of 2.6 cm). The data were then log transformed after the addition of the number 1.0 before analysis to normalize the data (Green and Montagna, 1996; Osborne, 2002).

SigmaPlot 12.3™ software was used to produce ternary, grid, and scatter graphs. Systat 13™ software was used to carry out principal component analyses (PCAs) with correlation matrix and varimax rotation on substrate composition (percentage of each size fraction); sediment carbon, nitrogen, Cu, and Zn concentrations; nematode and harpacticoid copepod abundance; water depth; and $U_{max,5}$ of the seabed.

RESULTS

Ternary plots based on the proportion of sand, silt, and clay revealed gravel-free sediment texture classifications for all 23 stations in BS between 2009 and 2014 (Figures 1 and 2). Sediment texture provided a classification system in lieu of traditional sedimentary summary statistical variables (*e.g.*, mean, standard deviation, median [phi], and skewness) that could not be derived from some sediment grain size distributions that were based on too few grain size classes (Flemming, 2000; Folk and Ward, 1957; Friedman, 1979; Pejrup, 1988; Shepard, 1954). A strong textural gradient was observed ranging from predominantly sand at the SE entrance to fine sediment in the upper basin. This sediment composition continuum represents a strong hydrodynamic-depositional gradient along the length of BS. Sediment texture in BS falls within six of the available 12 classes outlined in the ternary plot: sand, loamy sand, sandy loam, loam, silty loam, and silty clay loam (Figure 2). When considering the stations located along the central axis of the Sound, the proportion of sand decreased from 99% to 3% and the clay content increased from 1% to 37% with increasing distance from the SE Baynes Sound entrance. Although a similar trend was observed for the nearshore stations located along the 20-m bathymetric contour, the sediment composition often contained a slightly higher fraction of coarse material, likely influenced by the shoreline and detrital sources within this narrow Sound. For example,

Table 1. *Sediment classifications based on sediment grain size statistical parameters.*

Station	Sediment Texture	Arithmetic Mean (SD)	Sorting	Skewness
BS2	Mud	36.61 (5.25)	Very poorly sorted	Very finely skewed
BS5	Mud	33.11 (5.63)	Very poorly sorted	Very finely skewed
BS8	Mud	34.38 (1.68)	Very poorly sorted	Very finely skewed
BS11	Mud–muddy sand	72.92 (57.88)	Very poorly sorted	Very finely skewed
BS14	Sandy mud–muddy sand	201.47 (57.88)	Very poorly sorted	Very finely–finely skewed
BS17	Muddy sand–slightly gravelly sand	198.07 (14.97)	Poorly–moderately-well sorted	Very finely–coarsely skewed
BS20	Sand–slightly gravelly sand	342.40 (29.14)	Well–very well sorted	Very finely skewed–symmetrical
BS21	Sand–sandy gravel	1417.93 (585.33)	Poorly–moderately-well sorted	Very coarsely skewed
BS22	Sand–gravelly sand	740.28 (562.55)	Poorly–very well sorted	Very finely–very coarsely skewed

SD = Standard deviation

red-symbol stations (stations 1–9) located in the upper basin can be split into two groups: (1) subtidal central axis stations (2, 5, 8) with silty clay loam to silty loam sediment textures and (2) nearshore stations (1, 3, 4, 6, 7, 9) with loam to sand sediment textures (Figure 2).

Sediment texture derived from a sediment size spectrum spanning from clay to gravel shows a gradient along the central axis stations ranging from mud in the upper basin to sand-gravel at the southern entrance. The sorting and skewness attributes reveal (1) very poorly sorted muds within the upper basin (stations 2–8) that are skewed toward very fine material, (2) poorly to well sorted sand within a transition zone (stations 11–17) that are skewed mainly toward fines, (3) well-sorted sand characterized by symmetrical distribution (very well sorted) just inside the SE entrance, and (4) a combination of poorly to well-sorted sand and gravel located close to the shoreline within the entrance constricted by Mapleguard Point (Table 1).

Figure 3 shows a ternary diagram delineating 16 groups associated with varying hydrodynamic conditions and sand

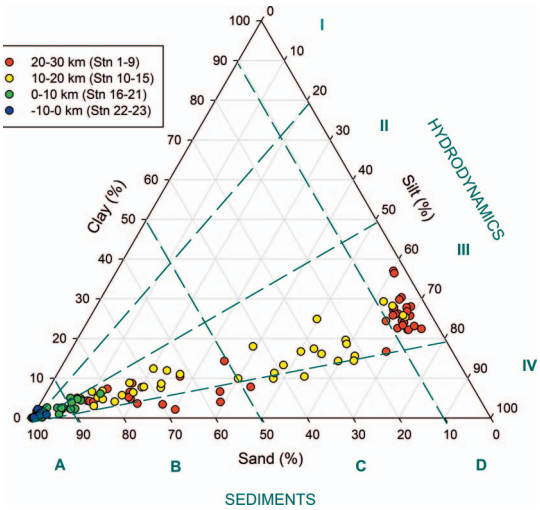

Figure 3. Ternary plot based on proportions of sand, silt, and clay overlaid with hydrodynamic (silt axis) and substrate-dominant (sand axis) classifications. Sampling stations are color-coded by station distance from the SE entrance of Baynes Sound, British Columbia. Hydrodynamic levels: I–IV; sand: A > 90%, 50% < B < 90%, 10% < C < 50%, D < 10%. The substrate texture falls predominantly within the high-energy hydrodynamic classification (III).

categories designed to identify different estuarine facies (Pejrup, 1988). The hydrodynamic classification consists of four categories (I–IV, from low to high energy) based on clay proportions that represent hydrodynamic conditions during deposition associated with the cumulative effect of current velocity, wave turbulence, and water depth. The sand classification component (categories A–D) reflects the following seabed sand proportions: (A) >90%; 50% < B < 90%; 10% < C < 50%; D < 10%. The sand-silt-clay ratios of the study samples fall predominantly within hydrodynamic classifications III and IV, indicating highly energetic depositional conditions that produce silt-dominated mud along the sand gradient rather than clay-dominated mud.

The sand-silt-clay ratios falling within the sand corner of the ternary plot (category A: >90% sand) span all of the four hydrodynamic categories (I–IV), representing very calm to energetic conditions (Figure 3). Flemming (2000) proposed that this category be combined into one category to represent a facies driven by uniform hydrodynamic conditions that result in the deposition of a sand-dominated substrate. The sand facies is represented by the blue and green stations located directly outside (stations 22, 23) and inside (stations 16–21) BS, respectively (Figure 3). These stations are connected by the influence of a strong tidal jet at the restricted SE entrance of BS. The mixed facies, as indicated by the yellow stations, is located within the midsection of BS and overlaps with the nearshore stations of the upper basin. The silt-dominated mud facies is made up of the central axis subtidal stations, identified by red symbols within the 0%–10% sand category.

Figure 4 shows peak values of water velocities ($U_{max,5}$) across BS with the largest speeds (>1 m s^{-1}) occurring in the shallow regions between Comox and northern Denman Island as well as within the vicinity of the narrow SE entrance to the Sound (between Mapleguard and Repulse points). A gradual increase in current speed can be seen along the central axis of BS starting from the wider, deeper upper basin (stations 5, 8: 0.17–0.19 m s^{-1}), along the central narrow channel (stations 11–17: 0.19–0.32 m s^{-1}), and through the constricted shallow-silled southern entrance (stations 20, 21: 0.75–0.77 m s^{-1}). The maximum velocity at the Sound head (station 2) is greater (0.26 m s^{-1}) than those of the deep-basin stations (5, 8), likely because of strong tidal influence from the restricted sandbar entrance, river outputs, or both.

Figure 5 shows the linkage between the $U_{max,5}$ (Figure 5A), location of stations along the central axis of BS (Figure 5B), and sediment texture categories associated with combined hydro-

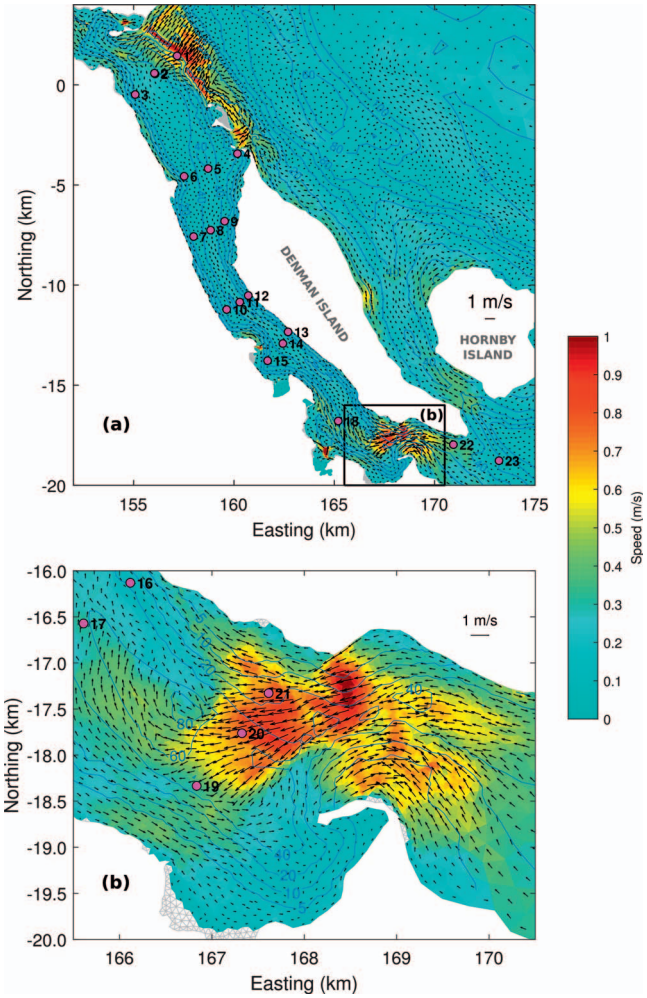

Figure 4. Modeled depth-averaged maximum hourly velocity values within 5 m above the seabed for the period from 1 June to 31 August 2012. The bathymetry contour lines are blue, sampling stations are designated by purple circles, and black arrows represent the direction and magnitude of water currents. The black arrows show an increase in water velocity toward the entrance of the Sound.

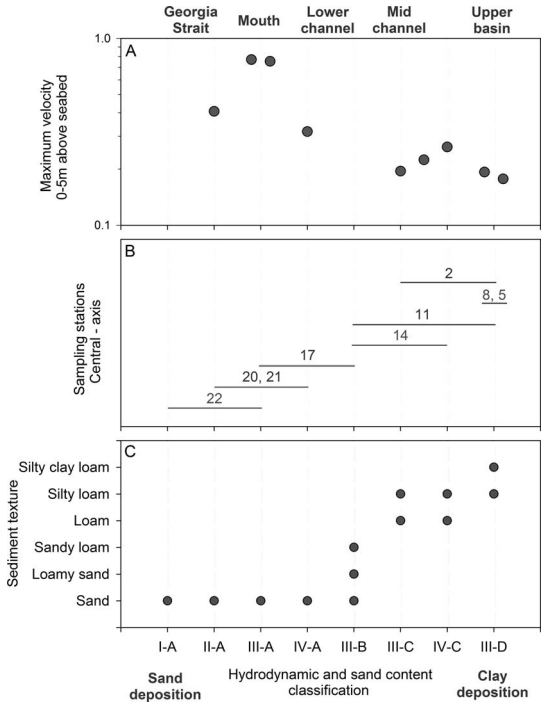

Figure 5. The relationship between depth-averaged maximum velocity within 5 m above the seabed (A), central axis stations at varying distances from the entrance of Baynes Sound (B), and hydrodynamic and sand content classification and sediment texture (C). Hydrodynamic levels: I–IV; sand: A > 90%, 50% < B < 90%, 10% < C < 50%, D < 10%. These graphs show the connections between sediment texture and associated hydrodynamic classifications and modeled velocity estimates.

dynamic-substrate categories (Figure 5C). The inner basin (stations 2–8) was characterized by sediment categories C–D, with sediment texture classifications ranging from silty clay loam to loam. The middle channel (stations 11–14) was characterized by sediment categories B–D, with sediment textures ranging from silty loam to loam. The lower channel (station 17) was characterized by sediment categories A–B, with sediment textures ranging from sandy loam to sand. The entrance stations (20–22) were characterized by sediment category A, with the sediment texture falling solely into one sediment texture category (A: sand).

Sediment porosity, organic carbon, and nitrogen content increased with increasing proportion of fine sediments along the length of BS (Figures 2 and 6). In contrast, sediment porewater sulfide values did not show a trend along the length of BS and fell mainly within the oxic-A category (0–700 μM) across all BS stations, with sediment texture categories ranging from sand to silty clay loam. Porewater sulfide classification levels were derived from eastern (Wildish *et al.*, 1999) and western (Sutherland *et al.*, 2007a) Canadian settings.

Sediment Zn and Cu concentrations were normalized with the reference element lithium to account for lithogenic influences associated with variations in mineralogy and granulometric variables within the seabed (Loring, 1990; Luoma, 1990; Qi *et al.*, 2010; Sutherland *et al.*, 2007b) (Figure 7A,B). Strong correlations were observed in the relationships between Li and Zn ($r^2 = 0.988$) as well as Li and Cu ($r^2 = 0.850$). In general, both sediment Zn and Cu concentrations increased with increasing distance from the SE entrance of BS, commensurate with decreasing grain size and increasing organic carbon content. Sediment Zn concentrations ranged between 10.7 and 121 μg g^{-1}, with all values falling below the Canadian sediment threshold effect level (TEL; 124 μg g^{-1}) (CCME, 1995, 1999b) (Figure 7B). Sediment Cu concentrations ranged between 4.0 and 65.2 μg g^{-1}, falling below the TEL (18.7 μg g^{-1}) and the probable effect level (PEL; 108 μg g^{-1}) (CCME, 1999a). In general, sediment Cu concentrations falling below TEL_{CU} were associated with the lower and outer reaches of BS.

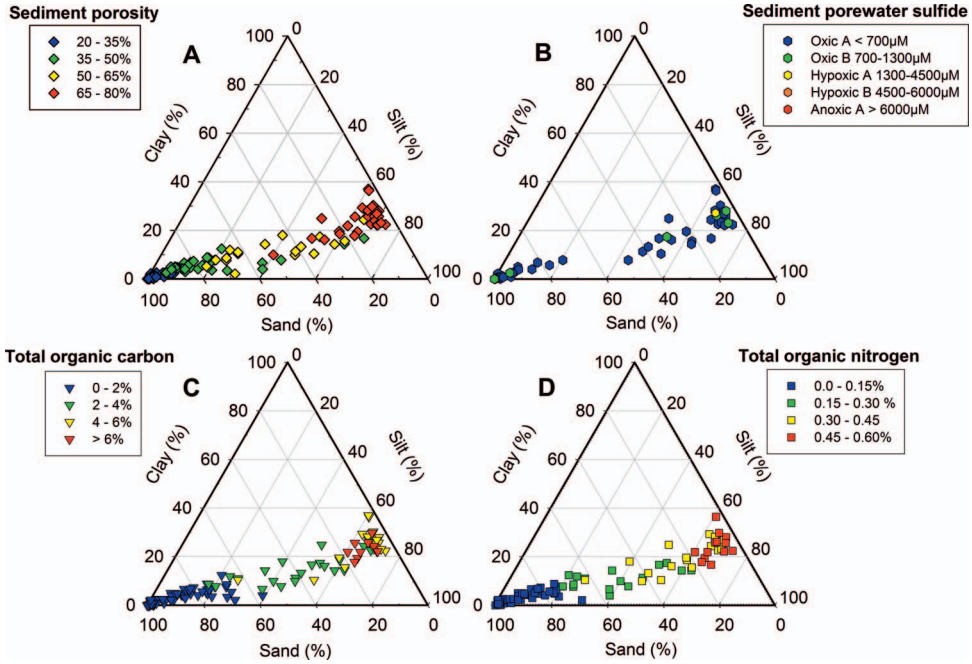

Figure 6. Ternary plots showing substrate texture of sampling stations categorized by sediment porosity (A), porewater sulfide concentration (B), organic carbon content (C), and organic nitrogen content (D). Although an increase in porous fine sediments is associated with higher organic content, sediment porewater sulfide does not vary in the same manner.

The relationship between nematode and harpacticoid copepod abundance revealed a slight increase in nematode abundance before reaching a plateau with increasing harpacticoid copepod abundance (Figure 8). Nematode abundance ranged between 2.72 and 203.25 nematodes cm^{-2} across BS, and the harpacticoid copepod abundance ranged between 0 and 32.45 nematodes cm^{-2}. The two meiofauna taxa were classified according to sediment texture categories (Figure 8A) and various levels of sediment organic carbon content (Figure 8B), sediment porosity (Figure 8C), and organic nitrogen content (Figure 8D). Harpacticoid copepods showed a stronger response to sediment properties compared with nematodes based on the larger range in harpacticoid copepod abundance. For example, harpacticoid copepods were not observed in the deep basin in the upper reach of BS (stations x, y, z) in sediments characterized by high silt, porosity, and organic carbon and nitrogen contents. Because the nematode abundance maintained a fairly stable abundance range across BS, the harpacticoid-copepod ratio increased as the abundance of harpacticoid copepods approached zero.

PCA factors describing meiofaunal distributions associated with substrate composition and geochemical attributes are presented in Figure 9. The statistical results revealed two distinct PCA factors: (1) fine sediment distribution characterized by geotechnical, organic, and meiofauna attributes (grey symbols) and (2) coarse sediment distribution characterized by $U_{max,5}$ and water depth (cyan symbols). The former factor accounted for 49% of the total variance, and the latter factor accounted for 19%.

DISCUSSION

Characterizing spatial patterns in seabed texture is an important component in understanding the evolution of sedimentary facies and estuarine bathymetry (Flemming, 2000; Pejrup, 1988). Estuaries are also known to be particle traps, where coarse to fine sediment gradients occur between a high-energy entrance and low-energy head of an estuary (Figure 2) (Schubel and Carter, 1984; Turner and Millward, 2002; Wei *et al*., 2007). BS is a macrotidal estuary that follows Fairbridge's (1980) concept that an estuary can be divided into three sections: (1) a lower reach that is predominantly marine and connected with the open sea, (2) a middle reach characterized by strong marine and freshwater mixing, and (3) a fluvial or upper reach experiencing freshwater outflows that establishes two-layer estuarine flow (Pickard, 1961). In this study, the sediment texture classifications along the central axis of BS support the aforementioned concepts with the following trends: (1) lower reach: sand to sandy loam; (2) middle reach: sandy loam to silty loam; and (3) upper reach: silty loam to silty clay loam (Figure 5). On application of Pejrup's (1988) hydrodynamic classification system, BS sediments were deposited under violent hydrodynamic conditions (III), supporting sand deposition in the lower reach and clay-silt deposition in the upper reach (Figure 3). These hydrodynamic classifications were conceptualized based on the observation that silt to clay proportions remained relatively constant across a sedimentary facie relative to that of sand and holds true in the BS system (Edwards and Frey, 1977; Fernandes *et al*., 2014; Pejrup, 1988, Shi, 1992). According to Pejrup (1988), hydrodynamic conditions during deposition reflect the com-

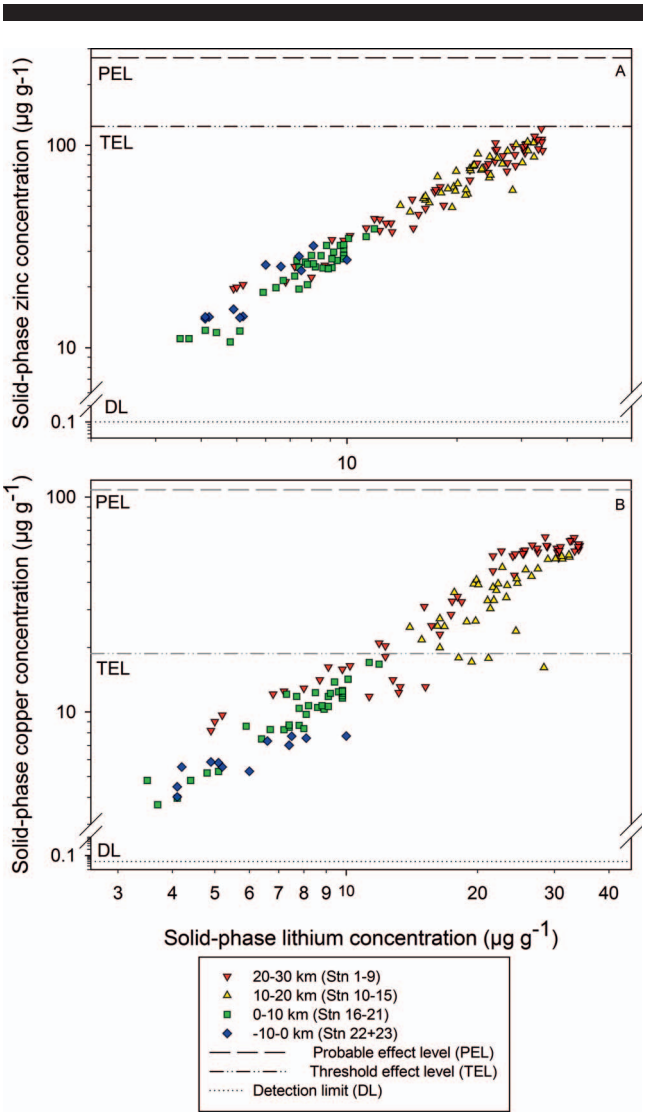

Figure 7. The relationship between solid-phase trace elements and lithium according to distance categories of sampling stations along the length of Baynes Sound. Both sediments Zn (A) and Cu (B) concentrations fell below the PEL (probable effect level) sediment quality guideline put forward by the Canadian Council of Ministers of the Environment (CCME 1999a,b).

bined effects of current velocity, wave turbulence, and depth and cannot be solely described by single traditional coefficients, such as Reynolds or Froude numbers. The dynamic nature of the hydrodynamic conditions in the lower and middle reaches of BS may carry fine particles from this area, inhibit flocculation and ETM processes, and minimize clay + silt accumulation within the seabed (Pejrup, 1988). In the upper fluvial reach of BS, the ETM and flocculation processes may either (1) scavenge clay and silt particles, increasing their retention in the water column, or (2) suppress this retention process because of the violent hydrodynamic conditions and deposit the clay/silt fraction within the deeper and calmer conditions of the basin. Sediment textural patterns observed in the current study within the depositional basin mirror those observed by Clague (1976). In general, sediment texture in BS appears to respond to a combination of factors, including (1) the proximity to terrestrial and river sources (Comox sandbar, landform sand bluffs; *e.g.*, Willemar Bluff; Clague, 1976), (2) river-marine interactions (particulate flocculation and ETM), (3) water depth (dampening of current velocities at deeper depths), and (4) the restricted SE entrance responsible for the down-Sound hydrodynamic gradient.

The alignment of a sandbar and tidal flow at the lower reach of the entrance identifies BS as a bar-built estuary that developed according to its geological and geomorphological features, as well as a balance between sedimentation and tidal processes (Pritchard, 1967). The high-velocity flows at the constricted SE entrance between Mapleguard and Repulse points are likely responsible for the deposition and maintenance of a well-sorted sand-dominated shallow shoal consisting of 95%–99% sand (stations 20 and 21; Figures 1 and 4). The second factor of the PCA revealed strong associations between (1) $U_{max,5}$ and the coarse sand fractions (0.5, 1.0, and 2.0 mm) that occur at the tidally constricted Comox Bar (NE) and Mapleguard (SE) entrances and (2) water depth and the fine sand fraction (0.105 mm). When considering the first association, the highest proportions of the 0.5- and 1.0-mm grain size fractions were observed at stations 1 (Comox Bar) and 20 and 21 (Mapleguard-Repulse points). This observation supports the notion that well-sorted sandy features develop from exposure to high-velocity conditions in which fine sediments are transported to calmer environments (Amos, 1974). The direct association between water depth and fine sand (0.105 mm) may represent the settlement of this grain size fraction in the deep basin in the upper reach of BS. The mixing of river and marine sources in this upper basin would likely facilitate flocculation and depositional processes that are influenced by the turbulence of water with fine sediment and organic material in the deep basin (Nair, Balchand, and Chacko, 1993; Pejrup, 1988). When considering the central axis stations, the sand-silt-clay ratios of the lower reach entrance and the upper reach basin that represent two extreme hydrodynamic conditions are associated with the least variation relative to that of the middle estuary section.

Seabed sediments play a role in biological and geochemical processes and can act as a repository for organic material and trace elements under certain hydrodynamic conditions (Dessai, 2008; Volvoikar *et al.*, 2014). In this study, a very strong association between fine sediments (clay, silt), sediment porosity, organic carbon content and nitrogen content, and trace elements (Zn, Cu) was observed in the first principal component that accounted for 49% of the total variance. In general, an increase in the proportion in fine sediments toward the head of the Sound resulted in increases in sediment porosity, organics, and trace element variables. Strong linkages between sediment grain size distribution, surface area, and consolidation processes (Hargrave *et al.*, 1997; Mayer, 1994), support the correlation between fine sediments and sediment porosity. In turn, these lower energy environments provide a medium for the accumulation of organic material that binds to sediment surfaces or collects within interstitial pore spaces (Fernandes *et al.*, 2014; Noronha-D'Mello and Nayak, 2015; Sutherland *et al.*, 2007a,b). The accumulation of organic

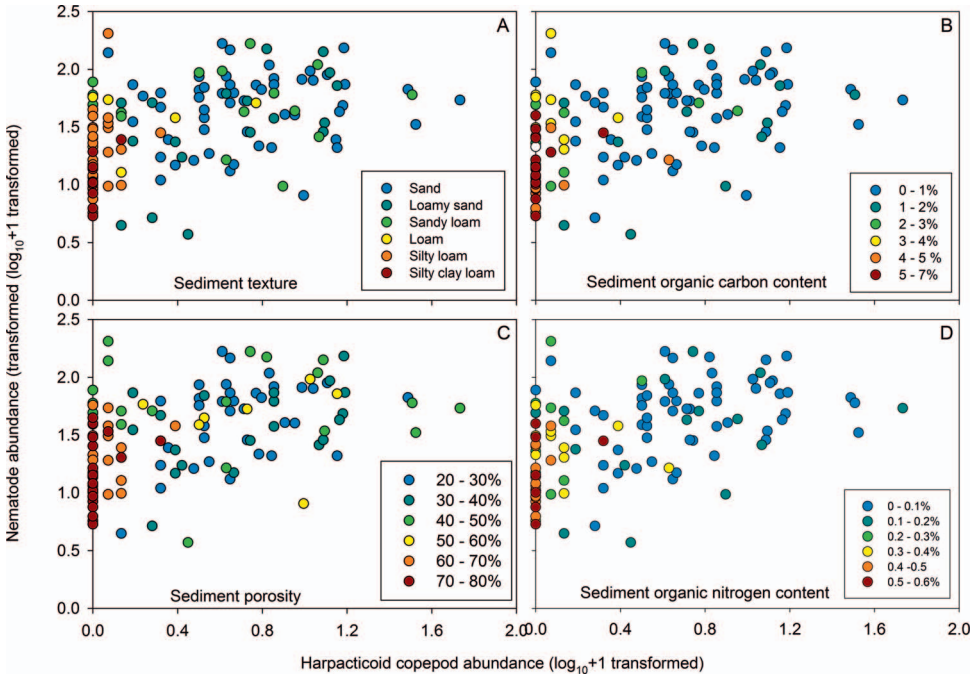

Figure 8. The relationship between nematode and copepod abundance categorized by sediment texture (A), sediment organic carbon content (B), sediment porosity (C), and sediment organic nitrogen content (D). The harpacticoid copepod abundance reaches zero for high-porous, organic-laden fine sediments.

material depends on the deposition, preservation, decomposition of various types of organic matter, or a combination of these factors (Yang *et al*., 2011). Potential sources of organic material in the deep basin of BS could arise from land runoff, riverine sources, flocculation of colloidal and inorganic material within an ETM, deposition of phytoplankton blooms, and anthropogenic inputs (Grimm and Gill, 1997; Turner and Millward, 2002). Although the deep basin in the upper reach of BS shows higher organic content than the middle or lower reaches, absolute organic carbon concentrations are relatively low. Furthermore, the observed sediment porewater sulfide values across the stations fell into the oxic category (96%) with the exception of a single Hypoxic-A classification at one station, suggesting low levels of benthic organic enrichment (Hargrave, Holmer, and Newcombe, 2008; Sutherland *et al*., 2007a). The generally low levels of organic carbon and porewater sulfide are likely a result of the violent (high-energy) hydrodynamic classification identified through the sediment texture (sand-silt-clay proportion) distribution within the Sound. Although ETM and flocculation processes scavenge clay and silt particles and enhance their retention in the water column, the energetic hydrodynamic conditions may suppress this process and make this clay + silt fraction available for deposition in the deeper and calmer conditions of the basin.

The abundance of trace elements such as Cu and Zn is closely linked to fine sediment and organic material, which typically reside in depositional zones associated with low-energy regimes (Clague, 1976; Dessai, 2008; Luoma, 1990; Noronha-D'Mello and Nayak, 2015; Sutherland *et al*., 2007b). Although trace elements naturally arise from fine sediments that contain metals within an aluminosilicate lattice structure and that have naturally endured weathering during transport from source rocks to estuarine environments (Maldonado and Stanley, 1981; Stanley and Liyanage, 1986; Volvoikar and Nayak, 2013), research has shown the significance of (1) organic coatings on fine particles as metal carriers that contribute to seabed trace element repositories (Ray *et al*., 2006; Stamoulis, Gibbs, and Menon, 1996) and (2) preferential accumulation in organic-rich settings where microbially mediated sulfate reduction promotes trace element retention as secondary metal sulfide phases (Emerson, Jacobs, and Tebo, 1983). In BS, the deeper central axis stations (2, 5, and 8) located in the upper basin show higher Zn and Cu concentrations relative to their nearshore counterpart stations (20-m bathymetric contour) as well as all of those stations located in the mid to low reaches. According to Clague (1976) and Waldie (1951), the upper basin bathymetry may be deep enough to escape the influence of strong seasonal outflows from the Courtenay River, as well as marine tidal exchanges spilling over the Comox sandbar, creating a low-energy depositional setting favoring mud flows and deposition.

Because trace elements can be used as indicators of estuarine quality, geonormalization techniques have been employed to account for anthropogenic inputs and naturally occurring variations associated with sediment grain size and organic coatings across a range of hydrographic and bathymetric settings (Calvert, 1976; Dessai, 2008; Noronha-D'Mello and Nayak, 2015; Sutherland *et al*., 2007b; Volvoikar and Nayak, 2013). The normalization technique involves correlating a trace element of interest with a trace element that represents a

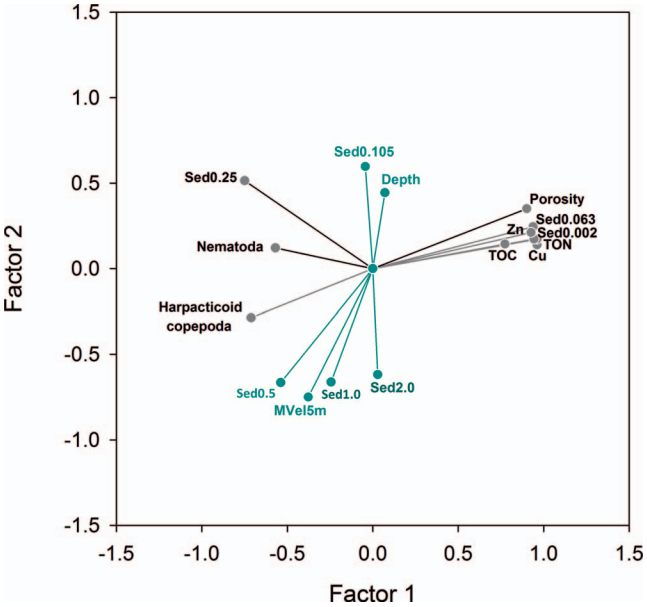

Figure 9. Vector plots showing the results of principal component analyses examining the relationships between sediment grain size, organic carbon and nitrogen content, trace element concentration (Cu, Zn), meiofauna abundance (nematodes, harpacticoid copepods), and maximum velocity at 5 m above the seabed in Baynes Sound. Factor 1 represents the accumulation of organic material and trace elements within porous fine sediments and the indirect relationship with meiofauna associated with a medium-sand substrate. Factor 2 represents the sediment texture gradient along the Sound where coarse sediments are associated with the high-velocity Sound entrance, and silt deposition is associated with the low-velocity deep basin at the head of the Sound.

conservative detrital element as a grain-size proxy (*e.g.*, Al, Fe, Li). Once the background regression is established, outliers that fall beyond the 95% confidence limits of the relationship are identified as anthropogenic), Both Al and Li have been used to normalize trace element concentrations, because they are conservative detrital elements enriched in fine-grained aluminosilicates (Calvert, 1976; Loring, 1990; Qi *et al.*, 2010; Volvoikar *et al.*, 2014). Lithium was used in this study because it produced a stronger correlation against a detrital background relative to that of Al, and has been used effectively in other British Columbia coastal settings characterized by similar sediment textures and facies (Figure 7) (Sutherland *et al.*, 2007b; Sutherland and Yeats, 2011).

Although anthropogenic contributions within fluctuating detrital background levels have been successfully identified using geonormalization techniques with Li (Aloupi and Angelidis, 2001; Ridgeway *et al.*, 2003; Yeats *et al.*, 2005), the lack of deviation from the normalized Zn *vs.* Li and Cu *vs.* Li regressions does not support an anthropogenic influence (Figure 7). Rather, the linear relationships of these ratios suggest that the concentrations of Cu and Zn reflect natural variability, with absolute concentrations being governed by variations in the relative proportions of different minerals that occupy different size classes. For example, the preferential enrichment of Cu and Zn in clays compared with that in sands is well defined and relates to the natural abundance of Cu and Zn in clay-size minerals (*e.g.*, chlorite) compared with sand-size minerals (*e.g.*, quartz and K feldspar) (Calvert, 1976; Wright, 1974).

In British Columbia coastal environments where sediment accumulation is dominantly governed by lithogenic inputs, background Cu concentrations have been shown to range from 35 to 110 $\mu g\ g^{-1}$ (Knight Inlet; McNee, 1997), consistent with the range for Cu abundance in terrigenous detritus, 60–120 $\mu g\ g^{-1}$ (Turekian and Wedepohl, 1961). Clague (1976) observed a Cu range of 4–74 $\mu g\ g^{-1}$ within the upper reaches of BS, which matches closely with the Cu concentration range observed across the entire Sound in the current study (4–65 $\mu g\ g^{-1}$). Sedimentary Zn concentrations in a lithogenic-dominated fjord (Knight Inlet) have been reported to range from 80 to 190 $\mu g\ g^{-1}$ (McNee, 1997). The sediment maxima observed for Cu (65 $\mu g\ g^{-1}$) and Zn (121 $\mu g\ g^{-1}$) in BS are less than the detrital maxima reported for Knight Inlet (McNee, 1997) and BS (Clague, 1976). Overall, the magnitude of the Cu (4–65 $\mu g\ g^{-1}$) and Zn (11–121 $\mu g\ g^{-1}$) values observed for BS and, importantly, the strong relationship to lithogenic proxies (Li) over the full concentration range strongly indicate that the variable abundances in BS can be attributed to natural textural variations in the local background.

Sediment criteria outlined in the Canadian Sediment Quality guidelines recommended by the Canadian Council of Ministers of the Environment (CCME, 1995) were applied to Zn and Cu concentrations observed in this study to determine the potential for biological effects in BS. The sediment guidelines consist of the TEL and the PEL, where adverse biological effects would rarely occur below the TEL guideline and likely occur above the PEL on exposure of biota to these trace element concentrations. In this study, sediment Zn concentrations fell below both the TEL (124 $\mu g\ g^{-1}$) and within range of background sediment Zn concentrations in British Columbia. With regards to Cu, although a proportion of values fell between the TEL (18.7 $\mu g\ g^{-1}$) and PEL (108 $\mu g\ g^{-1}$), the values fell within the range for detrital sediments observed in other British Columbia inlets (McNee, 1997). It is recognized that the total concentration of a metal in sediments is not a robust indicator of bioavailability (Vigneault and Gopalapillai, 2009); therefore, predicting the potential for adverse effects to benthic biota resulting from the observed Cu concentrations is challenging. Particulate Cu bioavailability in sediments depends on several variables, including the mineralogical (phase) associations, organic matter content, grain size, redox conditions, porewater pH, and individual taxon sensitivities and feeding strategies (Campbell *et al.*, 1988; Chapman and Wang, 2001; Luoma, 1990).

Meiofauna respond to physical and biochemical variations in the interstitial sedimentary setting because of their small size, potentially high abundances, rapid turnover rates, lack of larva dispersal, and asynchronous reproduction (Coull and Chandler, 1992; Higgins and Thiel, 1988). Harpacticoid copepod taxa have been considered to be more sensitive relative to nematode taxa in response to organic enrichment gradients (Amjad and Gray, 1983; Coull, Hicks, and Wells, 1981; Lambshead, 1984; Raffaelli, 1987; Raffaelli and Mason, 1981; Shiells and Anderson, 1985; Sutherland *et al.*, 2007a; Warwick, 1981). In this study, harpacticoid copepod abundance was indirectly

correlated with a geochemical gradient characterized by an increase in fine-grained sediments, porosity, and sediment organic and nitrogen contents toward the upper reach of the Sound (Figures 7 and 8). Because harpacticoid copepods are surface browsers, within their interstitial niche they may not be able to escape adverse organic-rich sedimentary conditions and take advantage of higher quality conditions in the water column, as can their calanoid and cyclopod counterparts (Raffaelli, 1987). Although nematodes were also indirectly associated with fine sediments and organic and trace element constituents, nematodes maintained a more consistent abundance across the geochemical gradient, with few data points dipping down to near-zero values (Figure 8). The PCA results show that nematodes and harpacticoid copepods align with a medium sand fraction (0.25 mm; Figure 9) that makes up the sandy loam (75% sand), loamy sand (80% sand), and sand (95% sand) textures associated with the highest meiofauna abundances (Figure 8). Other investigators have found that nematode community diversity responds to sediment composition, with some taxa-specific tolerances to different grain size and chemical attributes in the sedimentary environment (Armenteros *et al*., 2010; Essink and Keidel, 1998; La Rosa *et al*., 2001; Moreno *et al*., 2008; Schratzberger and Warwick, 1998a,b; Steyaert *et al*., 2003; Sutherland *et al*., 2007a; Warwick and Robinson, 2000). The weak relationship between nematode abundance and the observed geochemical gradient may include general nematode tolerance to osmotic stress regulating their water content with morphology and cuticular changes (Forster, 1998), a lack of a strong sediment porewater sulfide gradient that results in anoxic conditions that typify structures of nematode community diversity (Steyaert *et al*., 2007; Sutherland *et al*., 2007a), and the lack of nematode taxonomic resolution that would identify taxa with different (1) body types or modes of locomotion to accommodate various sediment textures and porosity and hydrodynamic regimes (Nichols, 1980; Ward, 1975), (2) resistance to organic enrichment and anoxic events (Moreno *et al*., 2008), and (3) feeding modes or guilds (Steyaert *et al*., 2003; Willems *et al*., 1982).

CONCLUSIONS

Sediment granulometry patterns followed a hydrodynamic gradient along the length of the central axis of BS. Six sediment texture classifications based on sand-silt-clay ratios were characterized in terms of their relationship with geochemical variables, meiofaunal attributes, and a velocity gradient. The upper depositional basin (stations 2–8) contained very poorly sorted sediments classified by a silty clay loam or mud fractions according to Pejrup (1988) and the Soi1 Classification Working Group (1998), respectively. The poorly sorted nature of the basin sediment is likely derived from the deposition of multiple sediment sources arising from contiguous fluvial, estuarine, and sandbar settings. The mid-sound transitional section (stations 11–14) of the BS estuary revealed the largest variation in both clay deposition categories (B, C, and D) and sediment texture classifications (very poorly sorted muds or sands). The substrate-scoured entryway of BS (stations 17–22) was characterized by a sand-gravel sediment mixture associated with a single clay deposition category (A) and $U_{max,5}$ values ranging between 0.32 and 77 m s^{-1}.

Sediment texture and hydrodynamic classifications can be used to characterize BS into three traditional sections according to Fairbridge's (1980) estuarine concept. Additionally, sediment along the central axis of BS may be characterized as a texture continuum driven by a single hydrodynamic classification (III; Pejrup, 1988) that promotes particle entrapment and accumulation of fine sediments, organic matter, and trace elements. Although a close association exists within the organic- and metal-laden fine sediments, the levels of Zn and Cu do not exceed the corresponding probable effects levels according Canadian sediment quality guidelines (CCME, 1995). In terms of meiofauna taxa, nematodes and harpacticoid copepods appeared to favor the medium sand fraction (0.25 mm) over the porous organic-laden fine sediments dominating the deep basin. The near-zero abundance of harpacticoid copepods within the deep organic-rich sediments suggests a greater sensitivity to these conditions relative to that of nematodes. The low sediment porewater sulfide concentrations (oxic classification; Hargrave, Holmer, and Newcombe, 2008) across the Sound do not follow the hydrodynamic sediment gradient, leading one to believe that existing benthic processes do not promote organic enrichment to the extent that facilitates anoxic events. Meiofauna taxa are likely structured predominantly by physical factors on a large spatial scale, while biological interactions play a large role on fine-scale distributions where certain taxa represent benthic environmental gradients or change (Maria *et al*., 2016; Zeppilli *et al*., 2015).

ACKNOWLEDGMENTS

We thank Nathan Blasco, Andrea Byrne, Hugh MacLean, Dan McPhee, Kate MacGivney, Steve Pace, Robyn Pearce, Shane Petersen, Scott Reid, Steve Romaine, Rapheal Roy-Jauvin, Krista Sandberg, Kenny Scozzafava, Andrea Sterling, and Kaitlin Yehle for their support during field work and laboratory analyses. Theraesa Coyle prepared the map for Figure 1. We also appreciate help from the Canadian Coast Guard crew aboard the CCGS *Vector* for all their support during the field program. This project was funded by the Program for Aquaculture Regulatory Research supported by Fisheries and Oceans Canada.

LITERATURE CITED

Aloupi, M. and Angelidis, M.O., 2001. Normalization to lithium for the assessment of metal contamination in coastal sediment cores from the Aegean Sea, Greece. *Marine Environmental Research*, 52(1), 1–12.

Amjad, S. and Gray, J.S., 1983. Use of the Nematode-Copepod Ratio as an Index of Organic Pollution. *Marine Pollution Bulletin*, 14(5), 178–181.

Amos, C.L., 1974. Intertidal Flat Sedimentation of the Wash-E. London: University of London, Ph.D. dissertation, 404p.

Arai, M.N. and Hay, D.E., 1982. Predation by medusa on Pacific herring (*Clupea harengus pallasi*) larvae. *Canadian Journal of Fisheries and Aquatic Sciences*, 39(11), 1537–1540.

Armenteros, M.; Perez-Garcia, J.A.; Ruiz-Abiemo, A.; Diaz-Asencio, L.; Helguera, Y.; Vincx, M., and Decraemer, W., 2010. Effects of organic enrichment on nematode assemblages in a microcosm experiment. *Marine Environmental Research*, 70, 374–382.

Blott, S., 2010. GRADISTAT version 8.0 for Excel versions 2007–2010. http://www.kpal.co.uk/GRADISTATv8xlsm.zip.

Bravender, B.A.; MacDougall, L.A.; Russell, L.R.; Beggs, C., and Miller, D.C., 2002. *Juvenile Salmon Survey, 1998, Courtenay River Estuary, Courtenay, B.C.* Canadian Technical Report Fisheries and Aquatic Science *2395*, 63p.

Calvert, S.E., 1976. The mineralogy and geochemistry of near-shore sediments. *In:* Riley, J.P. (ed.), *Chemical Oceanography*, 2nd edition. London: Academic Press, pp. 187–280.

Campbell, P.G.C.; Lewis, A.G.; Chapman, P.M.; Crowder, A.A.; Fletcher, W.K.; Imber, B.; Luoma, S.N.; Stokes, P.M., and Winfrey, M., 1988. *Biologically Available Metals in Sediments*. Ottawa, Ontario: National Research Council Canada, *NRCC No. 27694*, 295p.

Carpentier, A.; Como, S.; Dupuy, C.; Lefrançois, C., and Feunteun, E., 2014. Feeding ecology of *Liza* spp. in a tidal flat: Evidence of the importance of primary production (biofilm) and associated meiofauna. *Journal of Sea Research*, 92, 86–89.

Carswell, B.; Cheesman, S., and Anderson, J., 2006. The use of spatial analysis for environmental assessment of shellfish aquaculture in Baynes Sound, Vancouver Island, British Columbia, Canada. *Aquaculture*, 253(1–4), 408–414.

CCME (Canadian Council of Ministers of the Environment), 1995. *Protocol for the Derivation of Canadian Sediment Quality Guidelines for the Protection of Aquatic Life*. Ottawa, Ontario: Environment Canada, Guidelines Division, Technical Secretariat of the CCME Task Group on Water Quality Guidelines, *CCME EPC-98E*, 35p.

CCME, 1999a. Canadian sediment quality guidelines for the protection of aquatic life: Copper. *In: Canadian Environmental Quality Guidelines*. Winnipeg, Manitoba: Canadian Council of Ministers of the Environment, 4p.

CCME, 1999b. Canadian sediment quality guidelines for the protection of aquatic life: Zinc. *In: Canadian Environmental Quality Guidelines*. Winnipeg, Manitoba: Canadian Council of Ministers of the Environment, 4p.

Chapman, P.M. and Wang, F., 2001. Assessing sediment contamination in estuaries. *Environmental Toxicology and Chemistry*, 20(1), 3–22.

Chen, C.; Liu, H., and Beardsley, R.C., 2003. An unstructured, finite-volume, three-dimensional, primitive equation ocean model: Application to coastal ocean and estuaries. *Journal of Atmospheric and Oceanic Technology*, 20(1), 159–186.

Clague, J.J., 1976. *Sedimentology and Geochemistry of Marine Sediments near Comox, British Columbia*. Ottawa, Ontario: Energy, Mines and Resources Canada, *Geological Survey of Canada Paper 76-21*, 21p.

Coull, B.C. and Chandler, G.T., 1992. Pollution and meiofauna: Field, laboratory and mesocosm studies. *Oceanography and Marine Biology Annual Review*, 30, 191–271.

Coull, B.C.; Hicks, G.R.F., and Wells, J.B.J., 1981. Nematode/copepod ratios for monitoring pollution: A rebuttal. *Marine Pollution Bulletin*, 12(11), 378–381.

Dawe, N.K.; Buechert, R., and Trethewey, D.E.C., 1998. *Bird Use of Baynes Sound–Comox Harbour, Vancouver Island, British Columbia, 1980–1981*. Delta, British Columbia: Canadian Wildlife Service, Pacific and Yukon Region. *Technical Report Series No. 286*, 21p.

Dessai, D.V.G., 2008. Partition Geochemistry of Selected Elements of Sediments from Zuari Estuary, Goa, Central West Coast of India. Taleigão, Goa, India: Goa University, Ph.D. dissertation, 71p.

Diaz, R.J. and Rosenberg, R., 1995. Marine benthic hypoxia. A review of its ecological effects and the behavioural responses of benthic macrofauna. *Oceanography and Marine Biology*, 33, 245–303.

Duplisea, D.E. and Hargrave, B.T., 1996. Response of meiobenthic size–structure, biomass and respiration to sediment organic enrichment. *Hydrobiologia*, 339(1–3), 161–170.

Edwards, J.M. and Frey, R.W., 1977. Substrate characteristics within a Holocene saltmarsh, Sapelo Island, Georgia. *Senckenbergiana Maritimo*, 9, 215–259.

Emerson, S.; Jacobs, L., and Tebo, B., 1983. The behaviour of trace metals in marine anoxic waters: Solubilities at the oxygen-hydrogen sulfide interface. *In:* Wong, C.; Boyle, E.; Bruland, K.W.; Burton, J.D., and Goldberg, E.D. (eds.), *Trace Metals in Sea Water, Volume 9* (NATO Conference Series/IV Marine Sciences). Boston: Springer, pp. 579–608.

Essink, K. and Keidel, H., 1998. Changes in estuarine nematode communities following a decrease of organic pollution. *Aquatic Ecology*, 32(3), 195–202.

Fairbridge, R.W., 1980. The estuary: Its definition and geodynamic cycle. *In:* Olausson, E. and Cato, I. (eds.), *Chemistry and Biogeochemistry of Estuaries*. Chichester, United Kingdom: Wiley, pp. 1–36.

Fenchel, T., 1969. The ecology of marine microbenthos IV. Structure and function of the benthic ecosystem, its chemical and physical factors and the microfauna communities with special reference to the ciliated protozoa. *Ophelia*, 6(1), 1–182.

Fernandes, M.C.; Nayak, G.N.; Pande, A.; Volvolkar, S.P., and Dessai, D.V.G., 2014. Depositional environment of mudflats and mangroves and bioavailability of selected metals within mudflats in a tropical estuary. *Environmental Earth Sciences*, 72(6), 1861–1875.

Flemming, B.W., 2000. A revised textural classification of gravel-free muddy sediments on the basis of ternary diagrams. *Continental Shelf Research*, 20(10–11), 1125–1137.

Folk, R.L. and Ward, W.C., 1957. Brazos River bar: A study in the significance of grain size parameters. *Journal of Sedimentary Petrology*, 27(1), 3–26.

Forrester, C.R. and Ketchen, K.S., 1963. *A Review of the Strait of Georgia Trawl Fishery*. Ottawa, Ontario: Fisheries Research Board of Canada, *Bulletin 139*, 94p.

Forster, S.I., 1998. Osmotic stress tolerance and osmoregulation of intertidal and subtidal nematodes. *Journal Experimental Marine Biology and Ecology*, 22(1), 109–125.

Friedman, G.M., 1979. Differences in size distributions of populations of particles among sands of various origins: Addendum to IAS Presidential Address. *Sedimentology*, 26(6), 859–862.

Gage, J.D. and Bett, B.J., 2007. Deep-sea benthic sampling. *In:* Eleftheriou, A. and McIntyre, A. (eds.), *Methods for the Study of Marine Benthos*, Third Edition. Oxford, United Kingdom: Blackwell Scientific, pp. 273–325.

Green, R.H. and Montagna, P., 1996. Implications for monitoring: Study designs and interpretation of results. *Canadian Journal of Fisheries and Aquatic Sciences*, 53, 2629–2636.

Grimm, K.A. and Gill, A.S., 1997. Self-sedimentation of phytoplankton blooms in the geological record. *Sedimentary Geology*, 110(3/4), 151–161.

Hargrave, B.T.; Holmer, M., and Newcombe, C.P., 2008. Towards a classification of organic enrichment in marine sediments based on biogeochemical indicators. *Marine Pollution Bulletin*, 56(5), 810–824.

Hargrave, B.T.; Phillips, G.A.; Doucette, L.I.; White, M.J.; Milligan, T.G.; Wildish, D.J., and Cranston, R.E., 1997. Assessing benthic impacts of organic enrichment from marine aquaculture. *Water, Air, and Soil Pollution*, 99(1–4), 641–650.

Heip, C.; Vincx, M., and Vranken, G., 1985. The ecology of marine nematodes. *Oceanography and Marine Biology Annual Review*, 23, 399–489.

Higgins, R.P. and Thiel, H., 1988. *Introduction to the Study of Meiofauna*. Washington, D.C.: Smithsonian Institution Press, 488p.

Holmer, M.; Wildish, D., and Hargrave, B. 2005. Organic enrichment from marine finfish aquaculture and effects on sediment biogeochemical processes. *In:* Hargrave, B.T. (ed.) *Environmental Effects of Marine Finfish Aquaculture. Handbook of Environmental Chemistry, Volume 5M*. Berlin: Springer-Verlag, pp. 181–206.

Jamieson, G.S.; Chew, L.; Gillespie, G.E.; Robinson, A.; Bendell-Young, L.; Heath, W.; Bravender, B.; Tompkins, A.; Nishimura, D., and Doucette, P., 2001. *Phase 0 Review of the Environmental Impacts of Intertidal Shellfish Aquaculture in Baynes Sound*. Ottawa, Ontario: Canadian Science Advisory Secretariat, 103p.

Jay, D.A. and Musiak, J.D., 1994. Particle trapping in estuarine tidal flows. *Journal of Geophysical Research*, 99(C10), 20445–20461.

Jenkins, J.A.; Bravender, B.A.; Beggs, C.; Munro, B., and Miller, D., 2006. *The Distribution and Abundance of Juvenile salmonids and Other Species in the Courtenay River Estuary and Baynes Sound, 2000*. Nanaimo, British Columbia: Fisheries and Oceans Canada, Science Branch, Pacific Region, Pacific Biological Station, *Canadian Technical Report for Fisheries Aquatic Sciences*, *2659*, xiv + 77p.

La Rosa, T.; Mirto, S.; Mazzola, A., and Danovaro, R., 2001. Differential responses of benthic microbes and meiofauna to fish-farm disturbance in coastal sediments. *Environmental Pollution*, 112(3), 427–434.

Lacroix, D.I.; Boyd, S.; Esler, D.; Kirk, M.; Lewis, T., and Lipovsky, S., 2005. Surf scoters *Melanitta perspicillata* aggregate in association with ephemerally abundant polychaetes. *Marine Ornithology*, 33, 61–63.

Lambshead, P.J.D., 1984. The nematode/copepod ratio: Some anomalous results from the Firth of Clyde. *Marine Pollution Bulletin*, 15(7), 256–259.

Liu, H.; He, Q.; Wang, Z.; Weltje, G.J., and Zhang, J., 2010. Dynamics and spatial variability of near-bottom sediment exchange in the Yangtze Estuary, China. *Estuarine, Coastal and Shelf Science*, 86(3), 322–330.

Liu, X.; Huang, D.; Zhu, Y.; Chang, T.; Liu, Q.; Huang, L.; Zhao, W.; Lin, K., and Liu, L., 2015. Bioassessment of marine sediment quality using meiofaunal assemblages in a semi-enclosed bay. *Marine Pollution Bulletin*, 100(1), 92–101.

Loring, D.H., 1990. Lithium—A new approach for the granulometric normalization of trace metal data. *Marine Chemistry*, 29, 155–168.

Luoma, S.N., 1990. Processes affecting metal concentrations in estuarine and coastal marine sediments. *In:* Furness, R.W. and Rainbow, P.S. (eds.), *Heavy Metals in the Marine Environment*. Boca Raton, Florida: CRC Press, pp. 51–66.

Maldonado, A. and Stanley, D.J., 1981. Clay mineral distribution patterns as influenced by depositional processes in the southeastern Levatine Sea. *Sedimentology*, 28(1), 21–23.

Maria, T.F.; Vanaverbeke, J.; Vanreusel, A., and Esteves, A.M., 2016. Sandy beaches state of the art of nematode ecology. *Annals of the Brazilian Academy of Sciences*, 88(3), 1635–1653.

Mascart, T.; Lepoint, G.; Deschoemaeker, S.; Binard, M.; Remy, F., and De Troch, M., 2015. Seasonal variability of meiofauna, especially harpacticoid copepods, in *Posidonia oceanica* macrophytodetritus accumulations. *Journal of Sea Research*, 95, 149–160.

Mayer, L.M., 1994. Surface area control of organic carbon accumulation in continental shelf sediments. *Geochimica et Cosmochimica Acta*, 58(4), 1271–1284.

McKeague, J.A., 1978. *Manual on Soil Sampling and Methods of Analysis*, 2nd edition. Ottawa: Canadian Society of Soil Science, 212p.

McNee, J., 1997. The Post-Depositional Cycling of Cd, Cu, Mo and Zn in Several Hydrographically Distinct B.C. Fjords. Vancouver, British Columbia: University of British Columbia, Ph.D. dissertation, 285p.

Mirto, S.; La Rosa, T.; Danovaro, R., and Mazzola, A., 2000. Microbial and meiofaunal response to intensive mussel-farm biodeposition in coastal sediment of the western Mediterranean. *Marine Pollution Bulletin*, 40(3), 244–252.

Molinaroli, E.; Guerzoni, S.; De Falco, G.; Sarretta, A.; Cucco, A.; Como, S.; Simeone, S.; Perilli, A., and Magni, P., 2009. Relationships between hydrodynamic parameters and grain size in two contrasting transitional environments: The Lagoons of Venice and Cabras, Italy. *Sedimentology and Geology*, 219(1–4), 196–207.

Montagna, P.A.; Coull, B.C.; Herring, T.L., and Dudley, B.W., 1983. The relationship between abundances of meiofauna and their suspected microbial food (diatoms and bacteria). *Estuarine Coastal and Shelf Science*, 17(4), 381–394.

Moreno, M.; Ferrero, T.J.; Gallizia, I.; Vezzulli, L.; Albertelli, G., and Fabiano, M., 2008. An assessment of the spatial heterogeneity of environmental disturbance within an enclosed harbour through the analysis of meiofauna and nematode assemblages. *Estuarine Coastal and Shelf Science*, 77(4), 565–576.

Murrell, M.C. and Fleeger, J.W., 1989. Meiofauna abundance on the Gulf of Mexico continental shelf affected by hypoxia. *Continental Shelf Research*, 9(12), 1049–1062.

Nair, S.M.; Balchand, A.N., and Chacko, J., 1993. Sediment characteristics in relation to changing hydrography of Cochin estuary. *Indian Journal of Marine Sciences*, 22, 33–36.

Neira, C.; Sellanes, J.; Levin, L.A., and Arntz, W.E., 2001. Meiofaunal distributions on the Peru margin: Relationship to oxygen and organic matter availability. *Deep-Sea Research I*, 48, 2453–2472.

Nichols, J.A., 1980. Spatial pattern of a free-living marine nematode community off the coast of Peru. *International Review of Hydrobiology*, 65(2), 249–257.

Noronha-D'Mello, C.A. and Nayak, G.N., 2015. Geochemical characterization of mangrove sediments of the Zuari estuarine system, west coast of India, Part B. *Estuarine Coastal and Shelf Science*, 167, 1–13.

Osborne, J., 2002. Notes on the use of data transformations. *Practical Assessment Research and Evaluation*, 8(6), 1–7.

Pejrup, M., 1988. The triangular diagram used for classification of estuarine sediments; a new approach. *In:* de Boer, P.L.; Van Gelder, A., and Nio, S.D. (eds.), *Tide-Influenced Sedimentary Environments, and Facies. Sedimentology and Petroleum Geology*. Dordrecht, The Netherlands: D. Reidel, pp. 289–300.

Pickard, G.L., 1961. Oceanographic features of inlets in the British Columbia mainland coast. *Journal of the Fisheries Research Board of Canada*, 18(6), 907–999.

Pritchard, D.W., 1967. What is an estuary: Physical viewpoint. *In:* Lauff, G.H. (ed.), *Estuaries*. Washington, D.C.: American Association for the Advancement of Science, *AAAS Publication 83*, pp. 3–5.

Qi, S.; Leipe, T.; Rueckert, P.; Di, Z., and Harff, J., 2010. Geochemical sources, deposition and enrichment of heavy metals in short sediment cores from the Pearl River estuary, southern China. *Journal Marine Systems*, 82, S28–S42.

Raffaelli, D., 1987. The behaviour of the nematode/copepod ratio in organic pollution studies. *Marine Environmental Research*, 23(2), 135–152.

Raffaelli, D.G. and Mason, C.F., 1981. Pollution monitoring with meiofauna, using the ratio of nematodes to copepods. *Marine Pollution Bulletin*, 12(5), 158–163.

Ray, A.K.; Tripathy, S.C.; Patra, S., and Sarma, V.V., 2006. Assessment of Godavari estuarine mangrove ecosystem through trace metal studies. *Environmental International*, 32(2), 219–223.

Riddell, A. and Bryden, G., 1996. *Courtenay River Water Allocation Plan*. Nanaimo, British Columbia: BC Ministry of Environment, Lands and Parks, Regional Water Management, Vancouver Island Region, 80p.

Ridgeway, J.; Breward, N.; Langston, W.J.; Lister, R.; Rees, J.G., and Rowlatt, S.M., 2003. Distinguishing between natural and anthropogenic sources of metals entering the Irish Sea. *Applied Geochemistry*, 18(2), 283–309.

Schratzberger, M. and Warwick, R.M., 1998a. Effects of physical disturbance on nematode communities in sand and mud: A microcosm experiment. *Marine Biology*, 130(4), 643–650.

Schratzberger, M. and Warwick, R.M., 1998b. Effects of the intensity and frequency of organic enrichment on two estuarine nematode communities. *Marine Ecology Progress Series*, 164, 83–94.

Schubel, J.R. and Carter, H.H., 1984. The estuary as a filter for fine-grained suspended sediment. *In:* Kennedy, V.S. (ed.), *The Estuary as a Filter*. Orlando: Academic, pp. 81–105.

Schwinghamer, P., 1981. Characteristic size distributions of integral benthic communities. *Canadian Journal of Fisheries and Aquatic Sciences*, 38(10), 1255–1263.

Shepard, F.P., 1954. Nomenclature based on sand-silt-clay ratios. *Journal Sedimentary Petrology*, 24(3), 151–158.

Shi, Z., 1992. Application of the Pejrup Approach for the classification of the sediments in the microtidal Cyfi estuary, West Wales, U.K. *Journal of Coastal Research*, 8(2), 482–491.

Shiells, G.M. and Anderson, K.J., 1985. Pollution monitoring using nematode/copepod ratio: A practical application. *Marine Pollution Bulletin*, 16(2), 62–68.

Soi1 Classification Working Group, 1998. *Canadian System of Soil Classification*. Ottawa, Ontario: NRC Research Press, *Agriculture and Agri-Food Canada Publication No. 1646*, 3rd edition, 187p. (ISBN 0-660-17404-9).

Somerfield, P.J.; Warwick, R.M., and Moens, T., 2005. Meiofauna techniques. *In:* Eleftheriou, A. and McIntyre, A. (eds.), *Methods for the Study of Marine Benthos*, 3rd edition. Oxford, United Kingdom, Blackwell Publishing, pp. 229–272.

Stamoulis, S.; Gibbs, R.J., and Menon, M.G., 1996. Geochemical phases of metals in Hudson River estuary sediments. *Environmental International*, 22(2), 185–194.

Stanley, D.J. and Liyanage, A.N., 1986. Clay mineral variations in the northeastern Nile Delta, as influenced by depositional processes. *Marine Geology*, 73(3–4), 263–283.

Steyaert, M.; Moodley, L.; Nadong, T.; Moens, Y.; Soetaert, K., and Vincx, M., 2007. Responses of intertidal nematodes to short-term anoxic events. *Journal of Experimental Marine Biology and Ecology*, 345(2), 175–184.

Steyaert, M.; Vanaverbeke, J.; Vanreusel, A.; Barranguet, C.; Lucas, C., and Vincx, M., 2003. The importance of fine-scale, vertical profiles in characterising nematode community structure. *Estuarine Coastal and Shelf Science*, 58(2), 353–366.

Sun, X.; Zhou, H.; Hua, E.; Xu, S.; Cong, B., and Zhang, Z., 2014. Meiofauna and its sedimentary environment as an integrated indication of anthropogenic disturbance to sandy beach ecosystems. *Marine Pollution Bulletin*, 88(1–2), 260–267.

Sundulli, R. and De Nicola, M., 1991. Responses of meiobenthic communities along a gradient of sewage pollution. *Marine Pollution Bulletin*, 22(9), 463–467.

Sundulli, R. and De Nicola Giudici, M., 1989. Effects of organic enrichment on meiofauna: A laboratory study. *Marine Pollution Bulletin*, 20(5), 223–227.

Sutherland, T.F.; Levings, C.D.; Petersen, S.A.; Poon, P.A., and Piercey, B., 2007a. The use of meiofauna as an indicator of benthic organic enrichment associated with salmonid aquaculture. *Marine Pollution Bulletin*, 54(8), 1249–1261.

Sutherland, T.F.; Petersen, S.A.; Levings, C.D., and Martin, A.J., 2007b. Distinguishing between natural and aquaculture-derived sediment concentrations of heavy metals in the Broughton Archipelago, British Columbia. *Marine Pollution Bulletin*, 54(9), 1451–1460.

Sutherland, T.F. and Yeats, P.A., 2011. Elemental indicators of benthic organic enrichment associated with marine finfish aquaculture. *Dynamic Biochemistry, Process Biotechnology and Molecular Biology*, 5(Special Issue 1), 66–75.

Torres-Pratts, H. and Schizas, N.V., 2007. Meiofaunal colonization of decaying leaves of the red mangrove *Rhizophora mangle*, in southwestern Puerto Rico. *Caribbean Journal Science*, 43(1),127–137.

Turekian, K.K. and Wedepohl, K.H., 1961. Distribution of the elements in some major units of the Earth's crust. *Geological Society of America Bulletin*, 72, 175–192.

Turner, A. and Millward, G., 2002. Suspended particles: Their role in estuarine biogeochemical cycles. *Estuarine Coastal and Shelf Science*, 55(6), 857–883.

U.S. EPA, 1994. *Determination of Metals and Trace-Elements in Water by Ultrasonic Nebulization Inductively Coupled Plasma-Atomic Emission Spectrometry, Revision 1.2*. Cincinnati, Ohio: USEPA Office of Research and Development, *Methods for Determination of Metals in Environmental Samples – Supplement I. EPA/600/R-94-111*, 50p.

Vidakovic, J., 1983. The influence of raw domestic sewage on density and distribution of meiofauna. *Marine Pollution Bulletin*, 14(3), 84–88.

Vilas, F.; Bemabeu, A.M., and Mendez, G., 2005. Sediment distribution pattern in the Rias Baixas (NW Spain): Main facies and hydrodynamic dependence. *Journal of Marine Systems*, 54(1–4), 261–276.

Volvoikar, S.P. and Nayak, G.N., 2013. Depositional environment and geochemical response of mangrove sediments from creeks of northern Maharashtra coast, India. *Marine Pollution Bulletin*, 69(1–2), 223–227.

Volvoikar, S.P.; Nayak, G.N.; Mazumdar, A., and Peketi, A., 2014. Reconstruction of depositional environment of a tropical estuary and response of $\delta^{13}C_{org}$ and TOC/TN signatures to changing environmental conditions. *Estuarine Coastal and Shelf Science*, 139, 137–147.

Waldie, R.J., 1951. *Winter Oceanography of Baynes Sound and the Lazo Bight*. Nanaimo, British Columbia: Pacific Oceanographic Group, *Fisheries Research Board Canada, No. 441*, 15p.

Ward, A.R. 1975. Studies in the sublittoral free-living nematodes of Liverpool Bay. II. Influence of sediment composition on the distribution of marine nematodes. *Marine Biology*, 30(3), 217–225.

Warwick, R.M., 1981. The nematode/copepod ratio and its use in pollution ecology. *Marine Pollution Bulletin*, 12(10), 329–333.

Warwick, R.M. and Buchanan, J.B., 1970. The meiofauna off the coast of Northumberland. I. The structure of the nematode population. *Journal of Marine Biological Association of the United Kingdom*, 50(1), 129–146.

Warwick, R.M. and Robinson, J., 2000. Sibling species in the marine pollution indicator genus *Pontonema Leidy* (Nematoda: Oncholaimidae), with a description of *P. Metierranea* sp. nov. *Journal of Natural History*, 34(5), 641–662.

Webb, D.G., 1991. Effect of predation by juvenile Pacific salmon on marine harpacticoid copepods. I. Comparisons of patterns of copepod mortality with patterns of salmon consumption. *Marine Ecology Progress Series*, 72(1–2), 25–36.

Wei, T.Y.; Chen, Z.Y.; Duan, L.Y.; Gu, J.W.; Saito, Y.; Zhang, E.G.; Wang, Y.H., and Kanai, Y., 2007. Sedimentation rates in relation to sedimentary processes of the Yangtze estuary, China. *Estuarine Coastal and Shelf Science*, 71(1–2), 37–46.

Wildish, D.J.; Akagi, H.M.; Hamilton, N., and Hargrave, B.T., 1999. *A Recommended Method for Monitoring Sediment to Detect Organic Enrichment from Mariculture in the Bay of Fundy*. St. Andrews, Canada: Fisheries and Oceans Canada, *Canadian Technical Report of Fisheries and Aquatic Sciences No. 2286*, 31p.

Wildish, D.J.; Hargrave, B.T., and Pohle, G., 2001. Cost-effective monitoring or organic enrichment resulting from salmon mariculture. *ICES Journal of Marine Science*, 58(2), 469–476.

Willems, K.; Vincx, M.; Claeys, D.; Vanosmael, C., and Heip, C., 1982. Meiobenthos of a sublittoral sandbank in the southern bight of the North Sea. *Journal of Marine Biological Association of the United Kingdom*, 62(3), 535–548.

Wright, P.L., 1974. The chemistry and mineralogy of the clay fraction of sediments from the southern Barents Sea. *Chemical Geology*, 13(3), 197–216.

Yang, S.; Tang, M.; Yim, W.W.S.; Zong, Y.; Huang, G.; Switzer, A.D., and Saito, Y., 2011. Burial of organic carbon in Holocene sediments of the Zhujiang (Pearl River) and Changjiang (Yangtze River) estuaries. *Marine Chemistry*, 123(1–4), 1–10.

Yeats, P.A.; Milligan, T.G.; Sutherland, T.F.; Robinson, S.M.C.; Smith, J.A.; Lawton, P., and Levings, C.D., 2005. Lithium-normalized zinc and copper concentrations in sediments as measures of trace metal enrichment due to salmon aquaculture. *In:* Hargrave, B.T. (ed.), *Environmental Effects of Marine Finfish Aquaculture. Handbook of Environmental Chemistry, Volume 5M*. Berlin: Springer, pp. 207–220.

Zeppilli, D.; Jozée Sarrazin, J.; Leduc, D.; Arbizu, P.M.; Fontaneto, D.; Fontanier, C.; Gooday, A.J.; Kristensen, R.M.; Ivanenko, V.N.; Srensen, V.M.; Vanreusel, A.; Thébault, J.; Mea, M.; Allio, N.; Andro, T.; Arvigo, A.; Castrec, J.; Danielo, M.; Foulon, V.; Fumeron, R.; Hermabessiere, L.; Hulot, V.; James, T.; Langonne-Augen, R.; Le Bot, T.; Long, M.; Mahabror, D.; Morel, Q.; Pantalos, M.; Pouplard, E.; Raimondeau, L.; Rio-Cabello, A.; Seite, S.; Traisnel, G.; Urvoy, K.; Van Der Stegen, T.; Weyand, M., and Fernandes, D., 2015. Is the meiofauna a good indicator for climate change and anthropogenic impacts? *Marine Biodiversity,* 45: 505–535.